Particle Swarm Optimization Based Medical Image Segmentation Technique

Ahmed Afifi[*1], Toshiya Nakaguchi[*1], Norimichi Tsumura[*1], Yoichi Miyake[*1,*2]

Abstract

Accurate medical diagnosis requires a segmentation of a large number of medical images. Although the manual segmentation produces good results, it is a costly process (in the terms of money and time). On the other hand, the automatic segmentation is still challenging because of low image contrast and ill-defined boundaries. In this work, we propose a fully automated medical image segmentation framework. In this framework, the segmentation process is constrained by two prior models; a shape prior model and a texture prior model. The shape prior model is constructed from a set of manually segmented images using the principle component analysis (PCA) while the wavelet packet decomposition is utilized to extract the texture features. The fisher linear discriminate algorithm is employed to build the texture prior model from the set of texture features and to perform a preliminary segmentation. Furthermore, the particle swarm optimization algorithm (PSO) is used to refine the preliminary segmentation according to the shape prior model. In this work, we tested the proposed technique for the segmentation of the liver from abdominal CT scans and the obtained results show the efficiency of the proposed technique to accurately delineate the desired objects.

Keywords：medical image segmentation, shape priors, particle swarm optimization, liver segmentation

1. INTRODUCTION

However the medical image segmentation and the analysis of anatomical structure are very essential in medical diagnosis, it is very difficult and it requires a considerable amount of experience and knowledge. In the manual segmentation, the radiologist or the physician uses his/her experience to perform the segmentation, but when the amount of available data increased, the manual segmentation becomes a tough process and it is becoming essential to perform it automatically.

Many researchers attempt to automate the medical image segmentation process and several methods have been developed for this purpose [1], [2]. The traditional methods utilize the intensity changes in order to extract the edges and the local features of the desired objects [3] or they starts with a seed point inside the region of interest and then grows the region by using the similarity measures [4], [5]. Despite these

---

*1 Graduate School of Advanced Integration Science, Chiba University,
(1-33 Yayoi-cho, Inage-ku, Chiba 263-8522, Japan)
e-mail: afifi@graduate.chiba-u.jp
*2Research Center for Frontier Medical Engineering, Chiba University,
(1-33 Yayoi-cho, Inage-ku, Chiba 263-8522, Japan)

methods are helpful in some situations, they do not work well for medical applications because of noise, clutter, occlusion and the similarity between objects intensity.

more advanced and a state of the art methods model the segmentation problem as an optimization of energy function [6]. In these methods, a closed curve deforms until the balance is reached between the internal and the external energy. This curve is represented as a set of control points [7] or it is embedded as a zero level in a level set function [8]. Although these methods are more accurate than the traditional methods, the reliance on image information only usually leads to inadequate results. The addition of prior information to segmentation process has shown to improve the segmentation results and recently there has been an increased interest in the methods relying on prior information.

In this work, we propose an automated medical image segmentation framework incorporating both shape and texture prior. In this framework the desired texture is efficiently modeled using the wavelet packet decomposition. In addition, a prior shape model is constructed by the statistical analysis of a set of training shapes describing the variation in object shape. The particle swarm optimization algorithm (PSO) is used to accurately segment the image by adapting the prior shape model according to image features.

After this introduction, In Section2, we will describe in details the proposed segmentation technique. The experimental results will be presented in Section3 and the paper will be concluded in Section4.

2. THE PROPOSED FRAMEWORK

The proposed segmentation framework consists of two stages; offline training and online segmentation as shown in Figure. 2. In the training stage we apply the level set method [9] on a set of manually segmented images to represent the desired objects and then the prior shape model is derived using the principle component analysis. Additionally, in this stage we extract the wavelet-based textural features and employ the linear fisher discriminate algorithm [10] to build the textural prior model. In the segmentation stage, the PSO algorithm with inertia weight [11], [12] is utilized to segment the desired object from new CT scans according to its features and the previously constructed models.

2.1 The training stage

2.1.1 Prior shape model formulation.

Motivated by the pioneering work of Andy Tasi [13] et al., we derive the prior shape model from a set of n training images according to the following algorithm.

1. Derive the level set functions that describe the desired object from the n training images and denote it as $\Psi_i(x,y)\,, i=1,2,\dots,n$.
2. Compute the mean level set function $\overline{\Phi}$ from the set of level set functions Ψ_i as
$$\overline{\Phi}(x,y) = {}^{1}\!/_{n}\sum_{i=1}^{n}\Psi_i\,(x,y) \qquad (1)$$
3. Derive the shape variability functions $\widetilde{\Psi_i}, i=1,2,\dots,n$ as
$$\widetilde{\Psi_i}(x,y) = \Psi_i(x,y) - \overline{\Phi}(x,y) \qquad (2)$$
4. Construct a column vectors $\psi_i, i=1,2,\dots,n$ consisting of N samples of each $\widetilde{\Psi_i}$, $N = N_1 \times N_2$ is the image size, by stacking the N_2columns of $\widetilde{\Psi_i}$.
5. Define the shape variability matrix S as $S = [\psi_1 \quad \psi_2 \quad \cdots \quad \psi_n]$.
6. Employ the eigenvalue decomposition to the shape variability matrix S to compute the variance in shape as

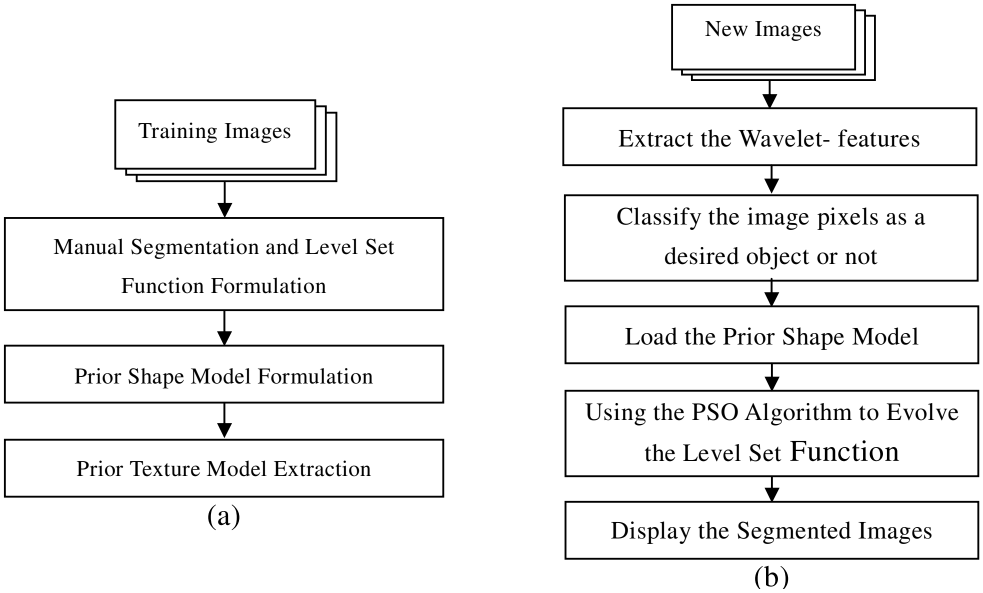

Fig. 1 The Proposed Technique; (a) the offline training stage, and (b) the online segmentation stage.

$$\frac{1}{n} SS^T = U\Sigma U^T \quad (3)$$

, where U is $N \times n$ matrix whose columns represent the n orthogonal modes of variation in shapes and $\Sigma = \text{diag}(\lambda_1, \lambda_2, \ldots, \lambda_n)$ is an $n \times n$ diagonal matrix whose diagonals elements represent the corresponding eigenvalues.

7. Arrange back the N elements of each column of U to yield a maximum of n eigenshapes or principle modes $\Phi_i, i = 1,2,\ldots,n$.

Sample training images and its level set representation are shown in Figure.2. The mean shape and the first three eigenshapes are illustrated in Figure.3.

2.1.2 Prior Texture Model Extraction

We utilize the over-complete wavelet packet transform [14] to extract the high-level feature vectors for each pixel in the training images. The over-complete wavelet packet transform doesn't perform the down-sampling as in standard wavelet packet transform, so it ensures the translation invariance property which is indispensable for textural analysis. In addition, it provides robust texture features at the expense of redundancy [15]. In this work, we extract the wavelet packet feature set by employing the following algorithm.

1. Apply a two-level over-complete wavelet packet decomposition on the input image.
2. At level-1, select the four sub-bands as feature sub-images.
3. At level-2, in each sub-channel, select the sub-band with the maximum variance to be a feature sub-image.

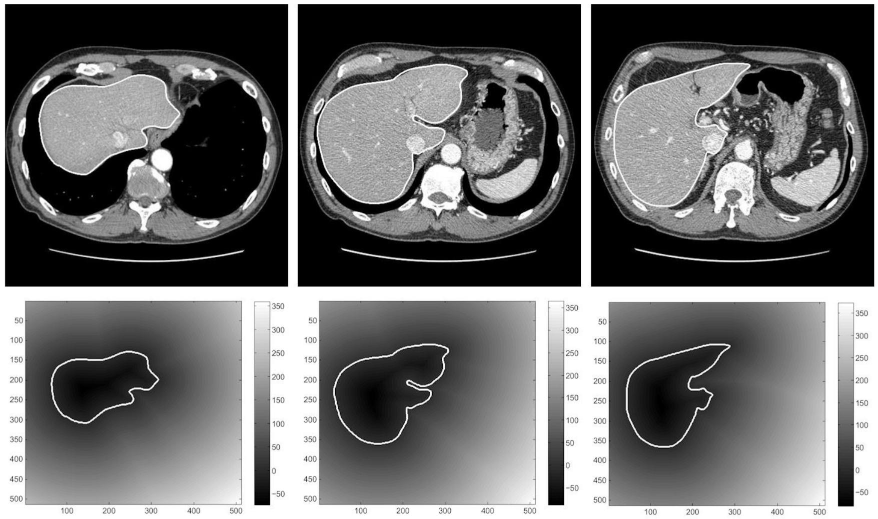

Fig. 2 sample training images, the manual segmentation on the top and its corresponding level set representation on the bottom.

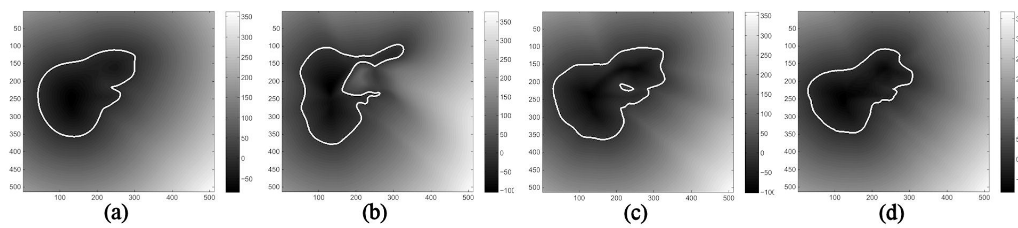

Fig. 3 shape model; (a) the mean shape (ms), (b) $ms + \sigma_1\Phi_1$, (c) $ms + \sigma_2\Phi_2$, (d) $ms + \sigma_3\Phi_3$, and $\sigma_i = \sqrt{\lambda_i}$

4. Calculate the local energy around each pixel of the feature sub-images as

$$E(x,y) = {}^{1}\!/_{(2m+1)^2} \sum_{i=-m}^{m} \sum_{j=-m}^{m} F(x+i, y+j) \tag{4}$$

   , where $F(x+i, y+j)$ is the wavelet coefficient of a feature sub-image in the $(2m+1) \times (2m+1)$ window centered at pixel (x,y).
5. Construct the feature vectors of each pixel in the image from the energy of the corresponding feature sub-images.

After the construction of the high level feature vectors, we assign a label for each pixel to indicate whether this pixel is a desired object pixel or not and finally, we use the linear fisher discriminate algorithm [10] to build the textural prior model.

2.2 The segmentation stage

The first step in the segmentation stage is to extract the wavelet packet based feature set of the new image and then classify each pixel in this image as a desired object pixel (true) or undesired object pixel (false) according to the prior textural model. This classification processes is carried out by using the linear fisher discriminate algorithm. Finally, this stage is completed by applying the PSO algorithm to get the level set function that truly segments the image as we will clarify in the next sections.

2.2.1 The Model Description

Each particle in the PSO population consists of the set of parameters that control the shape of the segmenting curve. As Tasi et al. did in [9], we use the mean shape and the shape variability derived from the training stage to define the level set function that implicitly represents the segmenting curve as in the following equation.

$$\Phi(x,y) = \bar{\Phi}(x,y) + \sum_{i=1}^{k} w_i \, \Phi_i(x,y) \qquad (5)$$

Where, k is the number of principle eigenshapes, $w_i, i = 1,2,\dots,k$ are the weights for these eigenshapes and these weights are ranged from $-\sigma_i \; to \; \sigma_i$ (where σ_i^2 are the eigenvalues corresponding to these i^{th} eigenshape). In addition, we consider the pose parameters; *a, b* for translation, *h* for scaling, and θ for the rotation angle, which incorporated in this framework using an affine transform. Therefore each particle *P* in the PSO population is represented as $P = [(w_i, i = 1,2,\dots,k), a, b, h, \theta]$ and it represents a segmenting curve. This segmenting curve can be expressed as the zero level of the level set function

$$\Phi(\tilde{x},\tilde{y}) = \bar{\Phi}(\tilde{x},\tilde{y}) + \sum_{i=1}^{k} \Phi_i\,(\tilde{x},\tilde{y}) \qquad (6)$$

where, $(\tilde{x},\tilde{y})$ is the new coordinate system obtained using the affine transformation.

The fitness of each particle in this work represents how the corresponding curve segments the image. So in the proposed technique, we tend to maximize the fitness function proposed in [16]. This fitness function is formulated as:

$$FT = 500(A + (1 - B)) \qquad (7)$$

Where, *A* is the fraction of pixels inside the segmenting curve that are labeled “true” and *B* is the fraction of the pixels outside the segmenting curve that are labeled “true”. The maximization of this fitness function means that more desired pixels are gathered inside the segmenting curve.

2.2.2 The PSO algorithm configuration

In this work, we are employing the PSO algorithm with inertia weight described in [11], [12]. The PSO algorithm includes an inertia term and acceleration constants which give us more control on the segmenting curve. The PSO algorithm configuration is shown in Table1 and the curve parameters configuration is practically selected and it can be adjusted according to the desired object. Our parameter configuration is provided in Table2.

2.2.3 The PSO algorithm implementation

After we configure the PSO algorithm and adjust the curve parameters according to the desired object, we carry out the segmentation process according to the following sequence:

1. Select the curve parameters randomly from the range specified in Table2 and create the corresponding level set functions.
2. Segment the image by using the curves derived from the generated level set functions.
3. Measure the fitness of each curve by computing the fitness function described in Section 2.2.1 and determine the best curve.
4. Update the curves parameters according to the PSO algorithm equations.

Table 1 PSO Algorithm configuration

Swarm Size (the number of segmenting curves)	25
The Maximum Number of Epochs	100
Local Best Influence	2
Global Best Influence	2
Initial Inertia Weight	0.9
Final Inertia Weight	0.4
Epoch When Inertial Weight at Final Value	80

Table 2 Curve Parameters Configuration

Parameter Name	Parameter Range	Maximum Velocity
$w_i, i = 1,2,\dots,k$	$-\sigma_i \sim \sigma_i$	$\sigma_i/5$
a, b	$-20 \sim 20$	2
h	$0.5 \sim 2$	0.5
θ	$-90 \sim 90$	10

5. Create the level set functions from the new parameters and repeat Step-2.
6. Repeat Step-3.
7. If the best curve is not changed for more than 10 epochs, produce the segmentation results; else go to Step-4.

3. EXPERIMENTAL RESULTS

We only illustrate the experiments of the liver segmentation from CT scans, but this technique can be adapted and implemented for the other organs. Here we employed and tested the proposed technique on a set of abdominal CT scans for five patients to segment the liver in these scans. Each CT scan consists of about 300 slices stacked together and the liver appears in about 30-50 slice. In this experiment, 34 slices of one patient in the dataset were manually segmented. The resulting level sets of manually segmented images were used to build the shape prior and textural prior models as described in Section2 and we practically select 10 principle modes to represent the shape variations ($k = 8$).

After we had built the shape and textural priors, we employed the proposed PSO segmentation technique on a set of slices of the patient used in the training stage and a set of slices for other patients. The resulting images shown in Figure.4 and Figure.5 illustrate the effectiveness of the proposed technique in liver segmentation from the CT scans.

Furthermore, we did another two experiments to segment the liver in the same set of slices and compare the results to show the effectiveness of the proposed technique. In the first experiment, we employ the active contour without edges method [17] with a manual initialization inside the liver and in the second experiment; we did the segmentation by using the wavelet packet decomposition feature set and the fisher linear discriminate algorithm. The goodness of fitness, G, of the segmentation results of all methods are computed and illustrated in Table.3.

To calculate the goodness of fitness, we generate two binary masks to represent the manual and the computerized segmentation results. These masks have a value of 1 inside the object and a value of 0 outside. Then the goodness of fitness is calculated according to the following equation.

$$G = \frac{|Am \cap Aa|}{|Am \cup Aa|} \quad (8)$$

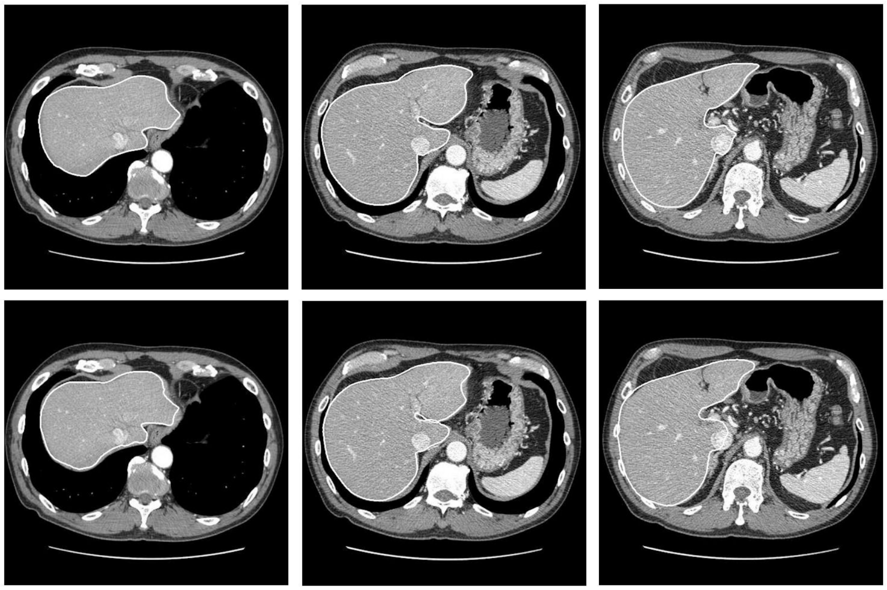

Fig. 4 proposed technique results on slices of the same patient used in the training stage, the manual segmentation on the upper row and the results on the bottom row.

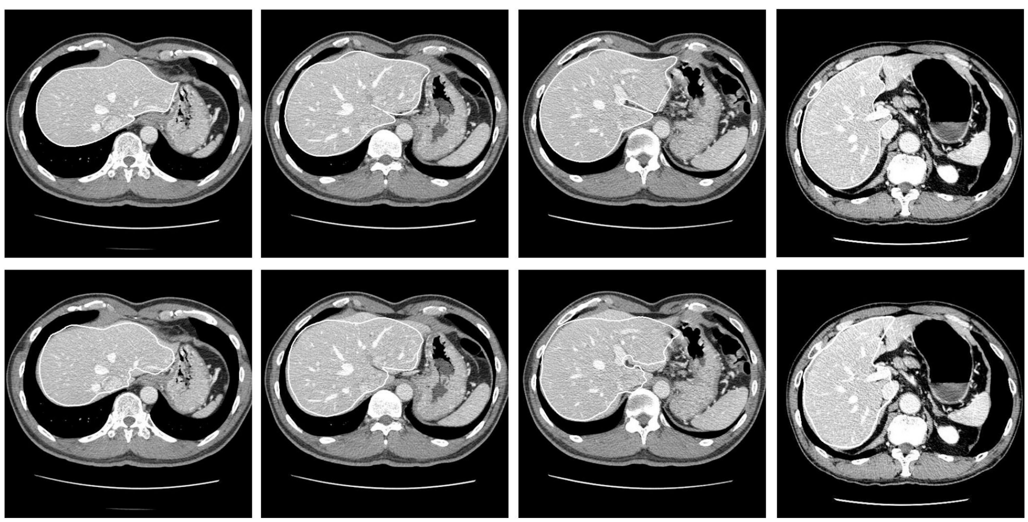

Fig. 5 proposed technique results on slices of patients other than the one used in the training stage, the manual segmentation on the upper row and the results on the bottom row.

Table 3 Goodness of fitness of the final segmentation results obtained using the different techniques.

The segmentation technique	G of the training slices	G of the test slices
The proposed technique	0.94	0.88
Active contour without edges	0.70	0.75
Wavelet packet decomposition	0.52	0.45

where, Am represents the area of manually segmented object and Aa represents the area of automatically segmented object . A score of 1 represents a perfect match with the manual segmentation. As illustrated in Table3, we note that the proposed PSO segmentation technique gives the best segmentation results. In addition, the proposed technique did not produce any overlap with the other objects as in the other methods.

4. CONCLUSION AND FUTURE WORK

In this work, the high level features extracted using the over-complete wavelet decomposition allows the technique to accurately discriminate the desired tissue. Also, the incorporation of prior shape model in the form of mean shape and shape variability as described in Section2 increases the ability to capture the desired object variations without overlapping with the other objects.

Furthermore, the utilization of the particle swarm optimization algorithm to evolve a region based level set function eliminates the need for deriving gradient of energy or solving complicated differential equations and it doesn't need level set re-initialization. Moreover, the PSO algorithm can efficiently explore the search space to converge to the desired object and its parameters can be easily adapted for any object. So the proposed PSO segmentation technique is very suitable for the segmentation of abdominal CT scans and it shows promised results.

In the future, we intend to enhance this PSO segmentation technique by employing the parallel PSO algorithm and extending the technique to the 3D cases .

References

[1] Bankman IN, hand book of medical imaging, processing and analysis, academic press, pp.67-211, 2000.

[2] Dzung LP, Chenyang X, and Jerry LP, "Current Methods in Medical Image segmentation", Annual Review of Biomedical Engineering, Vol.2, No.1., pp. 315-337, 2000.

[3] Chi Z, and Wang P, "A New Method of Color Image Segmentation Based on Intensity and Hue Clustering," icpr, p. 3617, 15th International Conference on Pattern Recognition (ICPR'00) – Vol.3, 2000.

[4] Pan Z, and Lu J, "A Bayes-Based Region-Growing Algorithm for Medical Image Segmentation," Computing in Science and Engineering, Vol.9, No.4, pp.32-38, Jul/Aug, 2007.

[5] Pohle R, and Toennies KD, "Segmentation of medical images using adaptive region growing", SPIE Medical Imaging, Vol.4322, pp.1337–1346, 2001.

[6] McInerney T and Terzopoulos D, "Deformable models in medical image analysis: a survey", Medical image analysis, Vol.1, No.2, pp.91-108, 1996.

[7] Kass M, Witkin A, and Terzopoulos D, "Snakes: Active contour models", international journal of computer vision, Vol.1, No.4, pp. 321-331, 1988.

[8] Osher S, and Fedkiw R, Level Set Methods and Dynamic Implicit Surfaces, Springer-Verlag, New York, 2003.

[9] Osher S, and Sethian J, "Fronts propagation with curvature dependent speed: Algorithms based on Hamilton-Jacobi Formulations", Journal of Computational Physics, Vol.79, pp.12-49, 1988.

[10] Franc V, and Hlavac V, "Statistical Pattern Recognition Toolbox for Matlab", Prague, Czech: Center for Machine Perception, Czech Technical University, 2004.

[11] Poli R, Kennedy J, and Blackwell T, “Particle Swarm Optimization: An Overview”, Springer Journal of Swarm Intelligence, Vol.1, pp.33-57, 2007.

[12] Clerc M, Particle Swarm Optimization, ISTE Ltd, 2006.

[13] Tasi A, Yezzi A, Wells W, and et al, “A Shape-Based Approach to the Segmentation of Medical Imagery Using Level Sets”, IEEE transaction on medical imaging, Vo.22, No.2, pp.137-154, 2003.

[14] Wang Q, and Feng D,” A Novel Texture Descriptor Using Over-Complete Wavelet Transform and Its Fractal Signature”, Lecture Notes in Computer Science, Vol.3568, pp.476-486. 2005.

[15] Li Y, Zhang Y, Jiang X, and et al, “Segmentation of Images Using Wavelet Packet Based Feature Set and Clustering Algorithm”, International Journal of Information Technology”, Vol.11, No.7, pp.112-121, 2005.

[16] Ghosh P, and Michell M, “Segmentation of Medical Images Using Genetic Algorithm”, Proceedings of the 8th annual conference on Genetic and evolutionary computation, pp.1171-1178, 2006.

[17] Chan TF, Vese LA, “Active Contour Without edges”, IEEE transactions on image processing, Vol.10, No.2, pp.266-277, 2001.

Abstract (Japanese)

画像診断においては目的の臓器などを特定する作業が伴う，つまり多数枚の医用画像からの形状抽出が必要である．医師が手作業で抽出することができれば最も正確な結果が得られるのだが，経済的・時間的コストの増大により実質的に不可能である．一方，計算機による自動抽出手法は様々提案されているが，医用画像の不鮮明さゆえに，いまだ未解決の問題とされている．そこで本論文では完全自動処理による新しい医用画像抽出フレームワークを提案する．このフレームワークは事前形状モデルと事前テクスチャモデルという二種類の事前知識モデルを用いている．事前形状モデルは手動抽出されたデータセットを主成分分析することで構築し，またウェーブレット分解を用いてテクスチャ特徴を算出する．前段の抽出処理においては，事前テクスチャモデルと算出したテクスチャ特徴からフィッシャーの線形判別子によって抽出を行う．さらに事前形状モデルと粒子群最適化手法(Particle Swarm Optimization)を用いて前段の抽出結果をさらに向上させる．本研究では，腹部 CT 画像から肝臓抽出することを目的として提案手法の検証を行った結果，目的の臓器をより正確に抽出できることが分かった．

Authors Biography

Ahmed Afifi received the B.Sc. from the faculty of science and the M.Sc. from the faculty of computers and information, Menoufiya University, Egypt in 2000 and 2005, respectively. He is currently pursuing the doctoral degree at Chiba University, Chiba, Japan.
His scientific interests include medical image analysis, pattern recognition, and optimization in vision.

Toshiya Nakaguchi received the B.E., M.E., and Ph.D. degrees from Sophia University, Tokyo, Japan in 1998, 2000, and 2003, respectively. Currently, he is an Assistant Professor of imaging science at the Graduate School of Advanced Integration Science, Chiba University, Chiba Japan. His current research interests include the computer assisted surgery and medical training, medical image analysis, real-time image processing, and image quality evaluation.

Norimichi Tsumura received the B.E., M.E. and D.E. in applied physics from Osaka University in 1990, 1992 and 1995, respectively. He moved to the Department of Information and Image Sciences, Chiba University in April 1995, as assistant professor. He is currently associate professor since 2002 at the Graduate School of Advanced Integration Science, Chiba University, Chiba Japan. He is interested in the color image processing, computer vision, computer graphics and biomedical optics.

Yoichi Miyake has been professor of Chiba University since 1989. He received Ph.D. from Tokyo Institute of Technology in 1978. During 1978 and 1979, he was a post doctoral fellow of Swiss Federal Institute of Technology (ETHZ). In 1997, he was a guest professor of University of Rochester. He was served as a president of SPSTJ (The Society of Photographic Science and Technology of Japan) from 2000 to 2002 and a vice president of IS&T (The Society for Imaging Science and Technology, USA) from 2000 to 2004. From 2003 to 2009, he was served as professor and director of Research Center for Frontier Medical Engineering in Chiba University. He is currently served as Research Professor in Chiba University.